Original Article

Association between diffusion-weighted imaging and tumor matrix in liver cancer: a cross-sectional study

Hans-Jonas Meyer[1], Johann Potratz[2], Dörthe Jechorek[2], Kai Ina Schramm[3], Jan Borggrefe[4], Alexey Surov[4]

[1]Department of Diagnostic and Interventional Radiology, University Hospital Leipzig, Leipzig, Germany; [2]Department of Pathology, Otto von Guericke University, Magdeburg, Magdeburg, Germany; [3]Department of Radiology and Nuclear Medicine, Otto von Guericke University, Magdeburg, Germany; [4]Department of Radiology, Mühlenkreiskliniken Minden, Ruhr-University Bochum, Bochum, Germany

Contributions: (I) Conception and design: HJ Meyer, A Surov; (II) Administrative support: J Borggrefe; (III) Provision of study materials or patients: J Potratz, D Jechorek, KI Schramm; (IV) Collection and assembly of data: J Potratz, D Jechorek, KI Schramm, J Borggrefe, HJ Meyer; (V) Data analysis and interpretation: HJ Meyer, A Surov; (VI) Manuscript writing: All authors; (VII) Final approval of manuscript: All authors.

Correspondence to: Hans-Jonas Meyer, MD. Department of Diagnostic and Interventional Radiology, University Hospital Leipzig, Liebigstraße 20, 04103 Leipzig, Germany. Email: Hans-jonas.meyer@medizin.uni-leipzig.de.

Background: Imaging modalities can reflect the underlying histopathology of tumors. However, the precise interactions between histopathological microstructure and the resulting imaging phenotype remain elusive. Predicting histopathological features, including the extracellular matrix, in a non-invasive manner could improve clinical care of liver tumors. The present study used cross-sectional guided biopsy specimens to utilize accurate spatial biopsy localization to correlate magnetic resonance imaging (MRI) derived the apparent diffusion coefficient (ADC) values with collagen IV expression in various liver cancers.

Methods: A total of 127 patients (n=68 female; 45.6%) with a mean age of 65.3±12.3 years were included in the analysis. Inclusion criteria were an available cross-sectional biopsy, available biopsy specimens and a pre-interventional MRI with diffusion-weighed imaging (DWI) sequence. The tumors included 45 patients (35.4%) with hepatocellular carcinoma (HCC), 26 patients (20.5%) with cholangiocellular carcinoma and 56 patients (44.1%) with liver metastases of various primary tumors. Prebioptic liver MRI with diffusion-weighted imaging was used to correlate ADC values with collagen IV expression obtained from liver biopsy. The ADC values were measured in a co-registered way with cross-sectional biopsy imaging to ensure the spatial concordance between imaging and histopathology. The stained area and signal intensity of the immunohistochemical staining were examined.

Results: The mean average stained area of collagen IV was 32.6%±27.4% and the mean staining intensity was 2.03±1.01. HCC showed statistically less stained area compared to the other tumor types (analysis of variance P<0.0001). In the overall patient sample, there was no correlation between ADCmean and average stained area (r=0.05, P=0.55) and staining intensity (r=–0.04, P=0.60). In a subgroup analysis of HCC patients, there was a significant correlation between ADCmin and the staining intensity (r=–0.33, P=0.02).

Conclusions: ADC values are not associated with collagen IV expression in liver tumors. The complex extracellular matrix is not reflected by the DWI signal, which can be discussed as mainly be influenced by the cellularity of the tumors. Further research is needed to investigate the complex interactions between histopathology and the resulting imaging phenotype of MRI for clinical care.

Keywords: Liver cancer; tumor matrix; diffusion-weighed imaging (DWI)

Submitted Aug 25, 2024. Accepted for publication Dec 16, 2024. Published online Mar 20, 2025.
doi: 10.21037/tcr-24-1516
View this article at: https://dx.doi.org/10.21037/tcr-24-1516

Introduction

Magnetic resonance imaging (MRI) can diagnose and characterize focal liver lesions. However, despite of increasing diagnostic capabilities and improved image quality, definitive histopathologic evaluation is still mandatory in most cases (1-4). However, liver biopsy procedure is an invasive procedure with a reported complication rate of 1% (5-7).

Therefore, extensive ongoing translational research efforts are investigating the possibility of non-invasive imaging modalities to predict histopathological features of tumors to reduce the need for histopathological evaluation.

Promising quantitative MRI methods can provide imaging markers, which are associated with cellularity, proliferation and other relevant features of tumors (8-14).

Among them, diffusion-weighted imaging (DWI) quantified by apparent diffusion coefficient (ADC) can reflect tumor cellularity and proliferative potential of tumors. The exact reasons for the ADC values of the tumors and the underlying tissue characteristics are complex (14-16). In most studies, cell count and cell sizes are emphasized as the tumor characteristics to reduce the water movement within the tumors (14-16). Large cell nuclei and large cell sizes lead to a reduction of the extracellular space, which is the part with the more free movement of the protons (14,17). However, the importance of the extracellular composition is widely discussed as the amount of extracellular matrix proteins can also reduce the free movement of the protons (18-20). However, this fact has only been investigated in *in-vitro* studies. Only few reports investigated the relationships between extracellular matrix and ADC values (21). In particular, the communication between tumor and matrix composition is of great importance, as the complex cellular cross-talk can lead to tumor suppression and tumor progression depending on the signaling pathways (22,23).

There is a clear clinical need to predict the underlying microstructure of tumors using imaging modalities. It could better provide image guidance for personalized treatments in a longitudinal fashion, whereas histopathology requires an invasive biopsy specimen that cannot be repeated multiple times. In addition, only imaging can provide information regarding about the entire tumor, whereas biopsy can only analyze a small part of the tumor. For example, the acquired specimen may be from a less aggressive tumor part and may not be representative of the entire tumor.

However, no study has investigated potential associations between the major extracellular matrix protein collagen IV and the ADC values using direct co-registration of the localization of the biopsy localization to ensure the correct associations between imaging and histopathology.

Therefore, the aim of this study was to elucidate possible associations between preinterventional MRI and bioptic specimen in liver cancer patients using exact spatial co-registration. We present this article in accordance with the STROBE reporting checklist (available at https://tcr.amegroups.com/article/view/10.21037/tcr-24-1516/rc).

Highlight box

Key findings

- Apparent diffusion coefficient values derived from diffusion-weighted imaging is not associated with Collagen IV-expression in different liver tumors.

What is known and what is new?

- The amount of extracellular matrix is debated to be an important factor influencing the magnetic resonance imaging signal of the diffusion-weighted imaging.
- With the present results, one can falsify this statement and assume that the cellularity is far more important in liver tumors.

What is the implication and what should change now?

- A complex study is needed to investigate different cellularity and extracellular matrix aspects in liver tumors to further investigate the interactions between imaging and histopathology.

Methods

The study was conducted in accordance with the Declaration of Helsinki (as revised in 2013). The study was approved by institutional ethics committee of the Otto von Guericke University, Magdeburg (approval number 43/20) and informed consent was waived from all individual participants due to the retrospective nature of the study.

This patient sample was previously evaluated in a study investigating ADC values and biopsy findings elsewhere (24).

Patients were included in this study if they met the following inclusion criteria:

- ❖ Pre-interventional MRI within 1 month before the biopsy.
- ❖ Available computed tomography (CT)- or MRI-guided liver biopsy images with documented position of biopsy needle;
- ❖ Lesion size >5 mm;
- ❖ Available pathologic specimens;

Exclusion criteria were: significant artifacts on pre-interventional MR images.

A total of 127 patients [68 (45.6%) women] with a mean

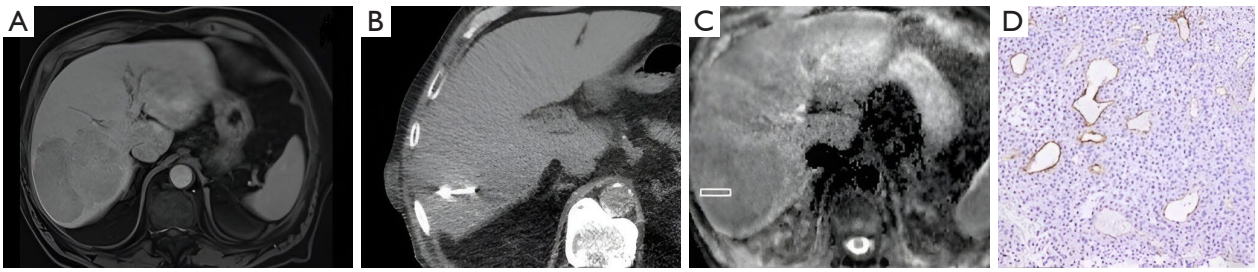

Figure 1 Representative case of the patient sample with a large tumor in the right liver lobe. (A) Portal-venous T1-weighted image with hypointense signal intensity of the tumor in the right liver lobe. (B) Axial slice of the computed-tomography-guided biopsy with display of the biopsy system centrally within the tumor. (C) Apparent diffusion coefficient-map and drawn region of interest of the biopsy region. The region of interest is highlighted by the white box. (D) Collagen-IV staining of the tumor. The magnification is 20-fold.

age of 65.3±12.3 years and a median age of 64.5 years were included in the present study. Due to the exploratory study design, sample size estimation was not possible.

The tumors included 45 patients (35.4%) with hepatocellular carcinoma (HCC), 26 patients (20.5%) with cholangiocellular carcinoma (CCC), 22 patients (17.3%) with liver metastasis of colorectal cancer (CRC), 20 patients (15.7%) with liver metastasis of breast cancer (BC), with 14 (11.0%) liver metastasis of pancreatic ductal adenocarcinoma (PDAC) (10.0%).

MRI

In all cases MRI was performed on a clinical 1.5-T scanner (Intera, Philips Healthcare, Hamburg, Germany). The imaging protocol included T2-weighted single-shot and turbo-spin echo sequences with and without fat suppression [repetition time (TR)/echo time (TE) =1,600:100]. Dynamic contrast-enhanced scans were obtained after administration of Gadolinium ethoxybenzyl-diethylenetriaminepentaacetic acid (0.1 mmol/kg body weight, Primovist®, Bayer HealthCare, Leverkusen, Germany): T1 weighted gradient echo sequences in the arterial, portal-venous and late venous phase as well as hepatobiliary phase 20 minutes after contrast media application. The parameters of the sequence were as follows: [TR 4 ms, TE 2 ms, Matrix 172×172, field of view (FoV) 345 mm × 345 mm, flip angle 10°]. The DWI was performed with a echo-planar imaging (EPI) sequence with respiratory triggering (TR/TE: 1959/59, FoV: 360 mm × 360 mm, matrix 144×142, b values of 0 and 600 s/mm^2, one repetition per b-value for b0 and 4 repetitions per b-value for b600, flip angle 90°) was obtained. The ADC maps were provided by the software.

All percutaneous biopsy procedures were performed by an experienced radiologists under sterile conditions using 18-Gauge coaxial needles during clinical routine. In each case, two to three cylindrical samples were obtained under CT- or MRI-guidance depending on the investigator's preference and the clinical situation.

Imaging analysis

MR images were analyzed within the clinical used picture archiving and communication system. The direct spatial correlation was performed with the subsequent CT- or MRI-guided biopsy. The region of interest (ROI) of the pretreatment MRI was placed at the last localization of the coaxial needle. The measurement was performed by a board-certified radiologist with 15 years of general experience. First, the images of the biopsy procedure were analyzed by the radiologists and the needle tip of the biopsy was determined Then, the radiologist drew a cylindrical ROI on the ADC map of each target lesion exactly corresponding to the needle position on the biopsy images to ensure high spatial correlation between imaging and histopathology. To improve the measurements, the post-contrast T1-weighted images were co-registered with the ADC maps to enhance the visualization between the sequences. All measurements were performed by an experienced board-certified radiologist with 16 years of experience in hepatobiliary imaging. ADCmean, ADCmin, and ADCmax values were estimated for all lesions. *Figure 1* provides a representative patient with the measurement.

Histological analysis with immunohistochemistry of Collagen IV expression

All biopsy specimens of the tumors were acquired before any form of treatment. In every case, the histopathology

was evaluated by two experienced pathologists (D.J., K.I.S.) in consensus blinded to patient or imaging data.

First, formalin-fixed, paraffin-embedded tissue serial sections (3 µm) were dewaxed in xylol and rehydrated by descending concentrations of ethanol. In every case, standard hematoxylin and eosin (HE) staining and following immunohistochemistry was performed. For antigen detection purposed, the automated immunohistochemistry slide staining system VENTANA BenchMark ULTRA (Roche Diagnostics GmbH, Mannheim, Germany), the VENTANA iVIEW DAB Detection Kit (Roche Diagnostics GmbH) and the indirect biotin-streptavidin method was used before the counterstaining with Haemalaun solution. Then, antigen retrieval was performed with proteinase 1 for 16 min, followed by incubation with specific primary antibody recognizing Collagen IV (polyclonal mouse antibody, clone CIV22; CellMarque, #239M-15), at 36 ℃ for 32 minutes, dilution 1:100. The stained area per high power field as well as the staining intensity were measured as outcome parameters. The protocol was performed according to the previous description (25).

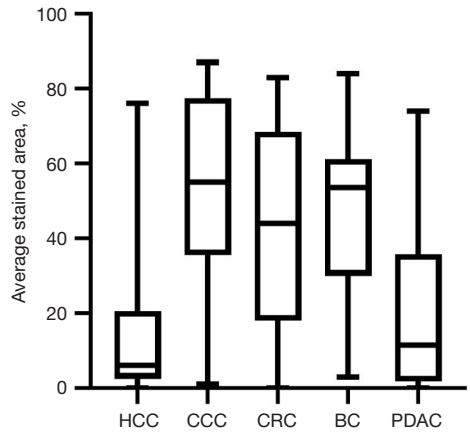

Figure 2 Box plot analysis to demonstrate the differences of the stained area in accordance to the tumor type. Hepatocellular carcinoma showed the lowest stained area with a mean of 13.5%±17.4% compared to 53.3%±24.8% for cholangiocellular carcinoma, 42.1%±26.7% for colorectal cancer, 47.0%±21.8% for breast cancer and 20.4%±22.0% for pancreatic ductal adenocarcinoma. BC, breast cancer; CCC, cholangiocellular carcinoma; CRC, colorectal cancer; HCC, hepatocellular carcinoma; PDAC, pancreatic ductal adenocarcinoma.

Statistical analysis

Statistical analysis and graphics creation were performed using GraphPad Prism 9 (GraphPad Software, La Jolla, CA, USA). Collected data were evaluated by means of descriptive statistics (absolute and relative frequencies). Spearman's correlation coefficient (r) was used to analyze associations between investigated parameters after testing for normality distribution with Kolmogorow-Smirnow test. In discrimination analysis of subgroups Mann-Whitney-*U* test was used. Analysis of variance (ANOVA) test was used to test for differences for all tumor types. In all instances, two-sided P values <0.05 were taken to indicate statistical significance.

Results

The mean average-stained area of collagen IV was 32.6%±27.4% and the mean staining intensity was 2.03±1.01.

There were differences of the stained area according to tumor type. HCC showed statistically lower stained area compared to the other tumor types (ANOVA P<0.001) with a mean of 13.5%±17.4% compared to 53.3%±24.8% for CCC, 42.1%±26.7% for CRC, 47.0%±21.8% for BC and 20.4%±22.0% for PDAC (*Figure 2*). For mean staining intensity CCC showed the highest intensity with a mean of 2.5±0.7 (ANOVA, P=0.01), which was statistically significant compared to PDAC with a mean of 1.5±1.1.

The descriptive statistics regarding the ADC values of the different tumors is given by *Table 1*.

Table 1 ADC parameters of the investigated tumors

ADC parameter	Overall sample	HCC	CCC	CRC	BC	PDAC	P value ANOVA
ADCmin $\times10^{-3}$ mm^2/s	0.72±0.23	0.78±0.22	0.75±0.27	0.67±0.23	0.64±0.13	0.60±0.20	0.03
ADCmean $\times10^{-3}$ mm^2/s	0.95±0.31	1.00±0.27	1.03±0.39	0.95±0.33	0.89±0.20	0.75±0.22	0.055
ADCmax $\times10^{-3}$ mm^2/s	1.26±0.36	1.34±0.33	1.33±0.44	1.23±0.37	1.15±0.28	1.06±0.29	0.057

Data are presented as mean ± SD. ADC, apparent diffusion coefficient; ANOVA, analysis of variance; BC, breast cancer; CCC, cholangiocellular carcinoma; CRC, colorectal cancer; HCC, hepatocellular carcinoma; PDAC, pancreatic ductal adenocarcinoma; SD, standard deviation.

Table 2 Correlation analysis between ADC parameters and the investigated matrix parameters in hepatocellular carcinoma patients

ADC parameters	Mean stained area		Mean staining intensity	
	r	P value	r	P value
ADCmin	–0.19	0.19	–0.33	0.02
ADCmean	–0.14	0.34	–0.22	0.14
ADCmax	–0.07	0.62	–0.03	0.81

ADC, apparent diffusion coefficient.

Table 3 Correlation analysis between ADC parameters and the investigated matrix parameters in cholangiocellular carcinoma patients

ADC parameters	Mean stained area		Mean staining intensity	
	r	P value	r	P value
ADCmin	0.26	0.19	–0.15	0.46
ADCmean	0.34	0.08	–0.16	0.42
ADCmax	–0.13	0.50	–0.19	0.34

ADC, apparent diffusion coefficient.

Table 4 Correlation analysis between ADC parameters and the investigated matrix parameters in metastasis of colorectal cancer patients

ADC parameters	Mean stained area		Mean staining intensity	
	r	P value	r	P value
ADCmin	–0.06	0.97	–0.06	0.78
ADCmean	0.07	0.72	0.14	0.51
ADCmax	–0.08	0.69	0.01	0.94

ADC, apparent diffusion coefficient.

Table 5 Correlation analysis between ADC parameters and the investigated matrix parameters in metastasis of pancreatic cancer patients

ADC parameters	Mean stained area		Mean staining intensity	
	r	P value	r	P value
ADCmin	0.01	0.96	0.17	0.54
ADCmean	0.09	0.74	0.25	0.37
ADCmax	0.15	0.58	0.37	0.18

ADC, apparent diffusion coefficient.

Correlation analysis

In the total patient sample, there was no correlation between ADCmean and average stained area (r=0.05, P=0.55) and stained intensity (r=–0.04, P=0.60). Similar results were found for ADCmin (r=–0.05, P=0.50 for stained area and r=–0.12, P=0.16 for stained intensity) and ADCmax (r=–0.03, P=0.71 for stained area and r=0.02, P=0.80 for stained intensity), respectively. The results of the correlation analysis are summarized in the *Tables 2-6*.

Table 6 Correlation analysis between ADC parameters and the investigated matrix parameters in metastasis of breast cancer patients

ADC parameters	Mean stained area		Mean staining intensity	
	r	P value	r	P value
ADCmin	0.01	0.98	0.03	0.98
ADCmean	0.15	0.50	–0.11	0.62
ADCmax	0.16	0.49	0.01	0.99

ADC, apparent diffusion coefficient.

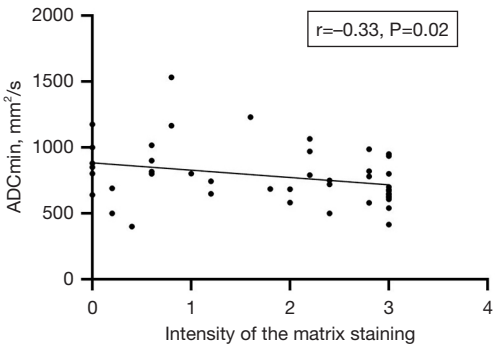

Figure 3 Spearman's correlation analysis between ADCmin and the intensity of the Collagen-IV staining in hepatocellular carcinoma patients (r=–0.33, P=0.02). ADC, apparent diffusion coefficient.

In subgroup analyses, the associations between ADC values and the collagen IV expression were analyzed according to the tumor entity. There was only one statistically significant correlation between ADCmin and the intensity of the staining in HCC patients (r=–0.33, P=0.02, *Figure 3*). No correlations were found for other tumor entities.

Discrimination analysis

Discrimination analysis was performed to test for differences between tumors with and without expression of collagen IV. In the HCC group, 6 tumors without collagen IV expression (13.3% of all tumors) were identified. The ADC parameters were not statistically different between these groups (ADCmean P=0.52, ADCmin P=0.11, ADCmax P=0.86).

Discussion

The present study investigated the associations between the ADC values of DWI and the expression of collagen IV, the major component of the extracellular matrix (26). This is an important investigation to further elucidate the complex interactions of the extracellular matrix on the proton motion measured by MRI.

It was shown that there was only a weak correlation between collagen expression and ADC values in CCC patients, whereas no correlation was found in liver metastasis. This reflects possible differences regarding the composition of the extracellular matrix in different liver tumors (27).

A key aspect of the present study was the accurate co-registration between the prebioptic imaging and the performed biopsy specimen to ensure the highest spatial correlation between imaging and histopathology. This approach is crucial to elucidate the complex interactions of the tumor microstructure resulting in the MRI phenotype.

There is no doubt that DWI quantified with ADC values can reflect the tumor biology in liver tumors and reflect the tumor microstructure (13-15). The inverse correlation with tumor cellularity was clearly stated in *in vitro* as well as human studies as shown in a large meta analysis (13). The main hypothesis is that the cellular space induces the slowest motion of the protons, whereas the protons have a higher diffusion in the extracellular space (18). This is explained by the fact that collisions of the protons with proteins and other structures does restrict the free movement of the protons. Membrane proteins have also been identified as important for proton diffusion and elevate the diffusion coefficient due to better permeability (28,29).

The extracellular space is composed of two main classes of extracellular macromolecules, the first group of macromolecules consists of polysaccharide chains called glycosaminoglycans that are linked to proteins in the form of proteoglycans and the second group of macromolecules consists of fibrous proteins (collagen and elastin) and fibrous adhesive proteins (fibronectin and laminin) (26,27).

In rat brain, the extracellular matrix is directly related to ADC values in an injury model (20). This was further elucidated in a human study with a strong inverse correlation between tissue collagen amount of the extracellular matrix in patients with esophageal cancer (21). The correlation coefficient reported by Aoyagi *et al.* reached r=–0.729, P=0.001 and was strongly inverse correlated with ADC values in this tumor (21).

In another study of glioma patients, hyaluronan staining was used to measure the amount of hyaluronan in these patients. The authors found a positive correlation between mean ADC values and the mean hyaluronan index (r=0.35, P<0.05) (19). Similar results have been reported in BC patients and in an *in vitro* model (30,31).

Interestingly, ADC values were also inversely correlated with collagen content in acute venous thrombosis (32).

However, it is not only important to understand the associations between ADC values and histopathology, but it may also have prognostic relevance. For example, the importance of collagen I expression in HCC patients has been extensively described (33-35). In a recent *in vitro* study liver cancer cell-matrix interaction induces cholangiocytic differentiation and switches liver cancer cells from a proliferative to an invasive phenotype through the Src/MAPK pathway (36). In another study, the expression of collagen IV and hyaluronic acid derived from preoperative serum levels were associated with liver function and prognosis (37).

In liver metastasis, the interactions between tumor cells and the extracellular matrix are of increasing interest (35,36). In CRC metastasis collagen IV is highly upregulated (36) and has been shown to have prognostic relevance (37). Furthermore, there are several metastatic growth patterns, that are associated with extracellular matrix composition and outcome (36). However, it was not possible in the current analysis to further investigate the metastatic growth pattern in the present cohort due to the biopsy design.

The present study is not free from limitations. First, it is a retrospective study with known inherent shortcomings. To overcome some bias, imaging and histopathological evaluation were blinded to each other. Second, the subgroups of liver metastases derived from pancreatic cancer and CRC are small. In addition, further subanalyses to adjust for histologic subtypes of primary tumors were not possible. In addition, tumor microstructure and extracellular matrix composition may differ according to tumor grade and subtype.

Conclusions

In contrast to published *in vitro* results, there were only weak associations between collagen expression as the major extracellular component and ADC values derived from MRI. Further studies are needed to elucidate the exact reasons for diffusion restriction in liver tumors based upon tumor characteristics.

Acknowledgments

None.

Footnote

Reporting Checklist: The authors have completed the STROBE reporting checklist. Available at https://tcr.amegroups.com/article/view/10.21037/tcr-24-1516/rc

Data Sharing Statement: Available at https://tcr.amegroups.com/article/view/10.21037/tcr-24-1516/dss

Peer Review File: Available at https://tcr.amegroups.com/article/view/10.21037/tcr-24-1516/prf

Funding: None.

Conflicts of Interest: All authors have completed the ICMJE uniform disclosure form (available at https://tcr.amegroups.com/article/view/10.21037/tcr-24-1516/coif). The authors have no conflicts of interest to declare.

Ethical Statement: The authors are accountable for all aspects of the work in ensuring that questions related to the accuracy or integrity of any part of the work are appropriately investigated and resolved. The study was conducted in accordance with the Declaration of Helsinki (as revised in 2013). The study was approved by institutional ethics committee of the Otto von Guericke University, Magdeburg (approval number 43/20) and informed consent was waived from all individual participants due to the retrospective nature of the study.

References

1. Ariff B, Lloyd CR, Khan S, et al. Imaging of liver cancer. World J Gastroenterol 2009;15:1289-300.
2. Llovet JM, Burroughs A, Bruix J. Hepatocellular carcinoma. Lancet 2003;362:1907-17.
3. McGlynn KA, Petrick JL, El-Serag HB. Epidemiology of Hepatocellular Carcinoma. Hepatology 2021;73 Suppl 1:4-13.
4. Haj-Mirzaian A, Kadivar A, Kamel IR, et al. Updates on Imaging of Liver Tumors. Curr Oncol Rep 2020;22:46.
5. Piccinino F, Sagnelli E, Pasquale G, et al. Complications following percutaneous liver biopsy. A multicentre retrospective study on 68,276 biopsies. J Hepatol 1986;2:165-73.
6. Neuberger J, Patel J, Caldwell H, et al. Guidelines on the use of liver biopsy in clinical practice from the British Society of Gastroenterology, the Royal College of Radiologists and the Royal College of Pathology. Gut 2020;69:1382-403.
7. McGill DB, Rakela J, Zinsmeister AR, et al. A 21-year experience with major hemorrhage after percutaneous liver biopsy. Gastroenterology 1990;99:1396-400.
8. Lambin P, Rios-Velazquez E, Leijenaar R, et al. Radiomics: extracting more information from medical images using advanced feature analysis. Eur J Cancer 2012;48:441-6.
9. Aerts HJ, Velazquez ER, Leijenaar RT, et al. Decoding tumour phenotype by noninvasive imaging using a quantitative radiomics approach. Nat Commun 2014;5:4006.
10. Incoronato M, Aiello M, Infante T, et al. Radiogenomic Analysis of Oncological Data: A Technical Survey. Int J Mol Sci 2017;18:805.
11. Meyer HJ, Hamerla G, Höhn AK, et al. CT Texture Analysis-Correlations With Histopathology Parameters in Head and Neck Squamous Cell Carcinomas. Front Oncol 2019;9:444.
12. Just N. Improving tumour heterogeneity MRI assessment with histograms. Br J Cancer 2014;111:2205-13.
13. Surov A, Meyer HJ, Wienke A. Associations between apparent diffusion coefficient (ADC) and KI 67 in different tumors: a meta-analysis. Part 1: ADC(mean). Oncotarget 2017;8:75434-44.
14. Surov A, Meyer HJ, Wienke A. Correlation between apparent diffusion coefficient (ADC) and cellularity is different in several tumors: a meta-analysis. Oncotarget 2017;8:59492-9.
15. Matsumoto Y, Kuroda M, Matsuya R, et al. In vitro experimental study of the relationship between the apparent diffusion coefficient and changes in cellularity and cell morphology. Oncol Rep 2009;22:641-8.
16. Tasaki A, Asatani MO, Umezu H, et al. Differential

diagnosis of uterine smooth muscle tumors using diffusion-weighted imaging: correlations with the apparent diffusion coefficient and cell density. Abdom Imaging 2015;40:1742-52.
17. Surov A, Caysa H, Wienke A, et al. Correlation Between Different ADC Fractions, Cell Count, Ki-67, Total Nucleic Areas and Average Nucleic Areas in Meningothelial Meningiomas. Anticancer Res 2015;35:6841-6.
18. Fornasa F. Diffusion-weighted Magnetic Resonance Imaging: What Makes Water Run Fast or Slow? J Clin Imaging Sci 2011;1:27.
19. Sadeghi N, Camby I, Goldman S, et al. Effect of hydrophilic components of the extracellular matrix on quantifiable diffusion-weighted imaging of human gliomas: preliminary results of correlating apparent diffusion coefficient values and hyaluronan expression level. AJR Am J Roentgenol 2003;181:235-41.
20. Vorísek I, Hájek M, Tintera J, et al. Water ADC, extracellular space volume, and tortuosity in the rat cortex after traumatic injury. Magn Reson Med 2002;48:994-1003.
21. Aoyagi T, Shuto K, Okazumi S, et al. Apparent diffusion coefficient correlation with oesophageal tumour stroma and angiogenesis. Eur Radiol 2012;22:1172-7.
22. Nazemi M, Rainero E. Cross-Talk Between the Tumor Microenvironment, Extracellular Matrix, and Cell Metabolism in Cancer. Front Oncol 2020;10:239.
23. Pickup MW, Mouw JK, Weaver VM. The extracellular matrix modulates the hallmarks of cancer. EMBO Rep 2014;15:1243-53.
24. Surov A, Eger KI, Potratz J, et al. Apparent diffusion coefficient correlates with different histopathological features in several intrahepatic tumors. Eur Radiol 2023;33:5955-64.
25. Ma HP, Chang HL, Bamodu OA, et al. Collagen 1A1 (COL1A1) Is a Reliable Biomarker and Putative Therapeutic Target for Hepatocellular Carcinogenesis and Metastasis. Cancers (Basel) 2019;11:786.
26. Nissen NI, Karsdal M, Willumsen N. Collagens and Cancer associated fibroblasts in the reactive stroma and its relation to Cancer biology. J Exp Clin Cancer Res 2019;38:115.
27. Naba A, Clauser KR, Ding H, et al. The extracellular matrix: Tools and insights for the "omics" era. Matrix Biol 2016;49:10-24.
28. Urushihata T, Takuwa H, Takahashi M, et al. Exploring cell membrane water exchange in aquaporin-4-deficient ischemic mouse brain using diffusion-weighted MRI. Eur Radiol Exp 2021;5:44.
29. Schob S, Surov A, Wienke A, et al. Correlation Between Aquaporin 4 Expression and Different DWI Parameters in Grade I Meningioma. Mol Imaging Biol 2017;19:138-42.
30. Kettunen T, Okuma H, Auvinen P, et al. Peritumoral ADC values in breast cancer: region of interest selection, associations with hyaluronan intensity, and prognostic significance. Eur Radiol 2020;30:38-46.
31. Reeves EL, Li J, Zormpas-Petridis K, et al. Investigating the contribution of hyaluronan to the breast tumour microenvironment using multiparametric MRI and MR elastography. Mol Oncol 2023;17:1076-92.
32. Gi T, Kuroiwa Y, Yamashita A, et al. High Signal Intensity on Diffusion-Weighted Images Reflects Acute Phase of Deep Vein Thrombus. Thromb Haemost 2020;120:1463-73.
33. Xiong YX, Zhang XC, Zhu JH, et al. Collagen I-DDR1 signaling promotes hepatocellular carcinoma cell stemness via Hippo signaling repression. Cell Death Differ 2023;30:1648-65.
34. Yuan RH, Hsu CL, Jhuang YL, et al. Tumor-matrix interaction induces phenotypic switching in liver cancer cells. Hepatol Int 2022;16:562-76.
35. Drew J, Machesky LM. The liver metastatic niche: modelling the extracellular matrix in metastasis. Dis Model Mech 2021;14:dmm048801.
36. Nyström H. Extracellular matrix proteins in metastases to the liver - Composition, function and potential applications. Semin Cancer Biol 2021;71:134-42.
37. Ueda J, Yoshida H, Mamada Y, et al. Evaluation of the Impact of Preoperative Values of Hyaluronic Acid and Type IV Collagen on the Outcome of Patients with Hepatocellular Carcinoma After Hepatectomy. J Nippon Med Sch 2018;85:221-7.

Cite this article as: Meyer HJ, Potratz J, Jechorek D, Schramm KI, Borggrefe J, Surov A. Association between diffusion-weighted imaging and tumor matrix in liver cancer: a cross-sectional study. Transl Cancer Res 2025;14(3):1764-1771. doi: 10.21037/tcr-24-1516

